Excited-State Proton Transfer as a Biological Probe. Determination of Rate Constants by Means of Nanosecond Fluorometry†

Michael R. Loken, John W. Hayes, James R. Gohlke, and Ludwig Brand*

ABSTRACT: Ionization constants of organic acids in the excited state may differ by several orders of magnitude from those observed in the ground state (Weller, A. (1961), *Progr. React. Kinet. 1*, 187). Nanosecond time-resolved fluorescence spectroscopy has been used to detect proton transfer in the excited state. It is shown that fluorescence lifetime data can be used to obtain the rate constants for excited-state proton transfer of 2-naphthol in aqueous solution. Three distinct methods are described for the calculation of rate constants, and good agreement is obtained between the values for rate constants obtained by these methods and those obtained with the steady-state approach. Rapid rates of excited-state proton transfer are found with 2,6-naphtholsulfonate in aqueous solution. When this chromophore is adsorbed to bovine serum albumin, little or no proton transfer is observed. The potential application of excited-state proton transfer to studies of biological macromolecules is discussed.

Differences in the chemical and physical properties of molecules in their excited states relative to their ground states can be used as the basis for designing probes of biological microenvironments. Organic acids exhibit excited-state ionization constants which differ by several orders of magnitude from those observed in the ground state (Förster, 1950a; Weller, 1961; Wehry and Rogers, 1966; Vander Donckt, 1970). Weller (1952), as well as other workers, has used steady-state fluorescence methods to calculate the forward and reverse rate constants for proton transfer. Rate constants for proton transfer depend on solvent environment and on the character of proton donors and acceptors. A quantitative measure of the environment of the probe can be made by calculating rates of proton transfer. These rates are expected to be sensitive to changes in protein conformation.

Quantitation of rate constants using kinetic methods yields the same values as those obtained by steady-state techniques using model compounds such as 2-naphthol. However, more information about the reacting system can be obtained by analysis of fluorescence decay curves, and such analysis can be applied to fluorescent probes attached to proteins. In this approach, light absorption and fluorescence are used as a relaxation technique to study reactions on a time scale of 10^{-9} sec or less. This type of relaxation technique differs from the traditional relaxation techniques in the extent of the perturbation. In excited-state studies the equilibrium is shifted by converting the reaction partners to new species (the excited state) rather than by changing intensive parameters such as the temperature or pressure.

Previous work (DeLuca *et al.*, 1971; Bowie *et al.*, 1972) has demonstrated the potential of excited-state proton transfer for investigating the active sites of enzymes. The aim of the present paper is to show how rate constants for excited-state proton transfer can be obtained from fluorescence lifetime measurements and to indicate the advantage of this approach over steady-state methods. A preliminary account of this work has been presented (Loken *et al.*, 1972).

Materials and Methods

2-Naphthol and 2,6-naphtholsulfonate monosodium salt were obtained from Eastman Organic Chemicals (Rochester, N. Y.) and were recrystallized three times from ethanol–water and water, respectively. The melting point of the purified 2-naphthol was 123°. The 2,6-naphtholsulfonate migrated as a single spot on silica gel thin-layer chromatography (Eastman chromagram sheets) in a solvent system of butanol–water–acetic acid in a ratio of 150:40:15.

All solutions were prepared with deionized water. Oxygen and carbon dioxide were removed from the solutions by bubbling nitrogen through the sample for 10 min. The pH was adjusted using HCl and was read on a Radiometer pH meter equipped with a scale expander. After degassing, the sample was placed in a Teflon-stoppered cuvet and sealed with parafilm.

Bovine serum albumin (crystallized 100%) was obtained from Mann Research Laboratories (New York) and was used without further purification. Solutions were prepared in 1×10^{-3} M sodium phosphate buffer (pH 7.3). Steady-state emission spectra were obtained using an Aminco-Keirs spectrophosphorimeter (Silver Spring, Md). The excitation wavelength for the steady-state spectra was 325 nm to minimize fluorescence due to tryptophan. Binding of 2,6-naphtholsulfonate to bovine serum albumin was measured using the method of Brand *et al.* (1967). A molecular weight of bovine serum albumin of 66,000 was used in the calculations.

Fluorescence lifetimes were measured on a single photon counting fluorometer similar to the one described by Schuyler and Isenberg (1971). Nuclear modules were made by Ortec (Oak Ridge, Tenn.) including timing filter amplifier 454, constant fraction discriminator 453, time-to-pulse-height converter 437A, and timing delay 425. A Hewlett-Packard (Santa Clara, Calif.) analog-to-digital converter and multi-

† From the Department of Biology and McCollum-Pratt Institute, The Johns Hopkins University, Baltimore, Maryland 21218. *Received June 14, 1972.* Supported in part by NIH Grant No. GM 11632 and American Cancer Society Grant No. P-610. Contribution No. 700 of the Department of Biology and McCollum-Pratt Institute. This investigation was supported (in part) by a Public Health Service Research Career Development award (GM 10245) from the National Institute of General Medical Sciences.

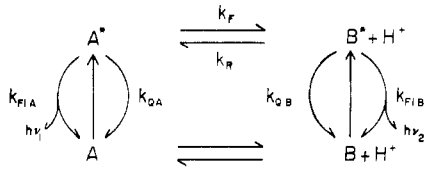

FIGURE 1: Kinetic scheme for excited-state proton transfer. A = protonated form; B = ionized form.

channel analyzer were interfaced with a Hewlett-Packard 2100 minicomputer. The electron multiplier phototube used was an Amperex (Hicksville, N. Y.) 56 DUVP operated at 2500 V. Correction for multiple photon events was made using the method of Coates (1968). A more detailed description of the instrumentation has been presented by Gohlke (1971).

A thyratron-pulsed lamp (Ware, 1971) run in air at 15 cm of Hg was used for excitation. The light was focused onto the sample through a 340-nm band-pass filter 340-38-32 (Baird-Atomic, Inc., Cambridge, Mass). The fluorescence emission was observed through a Bausch & Lomb 0.5-m monochromator (Rochester, N. Y.).

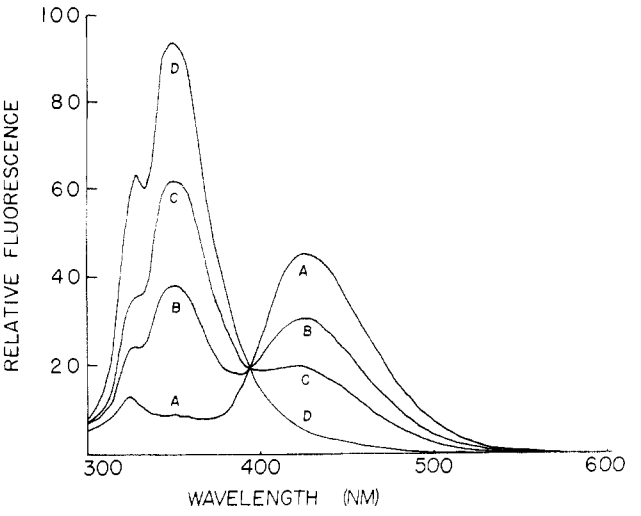

FIGURE 2: Uncorrected steady-state fluorescence emission spectra of 1×10^{-5} M 2,6-naphthosulfonate titrated with bovine serum albumin at pH 6.4 in 1×10^{-3} M sodium phosphate buffer. The curves were obtained at the following bovine serum albumin concentrations: (A) none; (B) 4×10^{-6} M, (C) 8×10^{-6} M, and (D) 20×10^{-6} M. Excitation wavelength is 325 nm. Isoemission point is 394 nm. Initial shoulder is due to scatter of exciting light.

Results

Weller has proposed a simple kinetic scheme for excited-state proton transfer (Figure 1). A and B represent the protonated and ionized forms of the chromophore, while A* and B* represent these species in the excited state. If the pK of the ground state differs from that of the excited state, the equilibrium between the two species will shift after excitation. One system which exhibits excited-state proton transfer is 2-naphthol in which both the ionized and the protonated forms fluoresce with emission peaks of 360 nm for the naphthol and of 425 nm for the naphtholate. The pK of the ground state is 9.46 while that of the excited state is 2.81 (Weller, 1961).

Following the excitation of a solution in which only A is present in the ground state, numerous competitive processes will tend to depopulate the first excited singlet state of A*. The absorbed energy may be lost either by the emission of a photon with a rate constant of k_{F1A} or by a variety of nonradiative transitions with a combined rate constant of k_{QA}. In addition, A* can lose a proton to its environment to produce B* provided the rate of this transfer (k_F) is on the same time scale as the other rates. Since no B exists in the ground state prior to excitation, any emission from B* must be due to a proton transfer reaction during the excited state. Similarly, B* will be depopulated by either fluorescence (k_{F1B}), quenching (k_{QB}) or by combining with a proton to regenerate A* with a second-order rate constant of k_R.

2,6-Naphtholsulfonate also exhibits excited-state proton transfer, but the rate of ionization is so fast that ionization is almost complete during the lifetime of the excited state. In water at pH 6.0, nearly all of the light emission occurred from the excited naphtholate as can be seen in the steady-state emission spectra (Figure 2A). A dramatic shift in the fluorescence emission from the ionized to the protonated form was observed when bovine serum albumin was added to the solution (Figure 2B and 2C). When an excess of bovine serum albumin was present (Figure 2D) there appeared to be no fluorescence from the ionized species. The isoemissive point at 394 nm suggests that only two forms are present, the adsorbed protonated form and the free, predominantly ionized form. Fluorescence titrations indicated that a 1:1 molar complex was formed with an association constant greater than 10^6 M^{-1}.

When a probe is bound to a protein, the change in environment may be reflected in a change in fluorescent properties. When 2,6-naphtholsulfonate is bound to bovine serum albumin, the shift in emission from the ionized to the protonated form indicates either there is no proton acceptor on the protein within the vicinity of the ionizing group and that solvent is excluded or that the rate of reprotonation is made very fast by a proton donor on the protein. Calculation of the rate constants for excited-state ionization of a chromophore bound to a protein would provide a quantitative measure of the proton accepting and donating characteristics of the binding site. This is a conceptually different approach than that used with other fluorescent probes in the characterization of microenvironments and may possibly lead to an identification of certain proton donors or acceptors at the binding site.

The kinetics of the transformation of naphthol into naphtholate in the excited state can best be visualized by nanosecond time-resolved emission spectra (Figure 3). By obtaining decay curves at several different wavelengths, emission spectra can be generated at discreet times during the fluorescence decay. The change in emission maxima as a function of time reflects the change in the relative amounts of the two species during the time period of emission. The relative amount of either species at any time is dependent on both the rate of interconversion as well as the rates of return to the ground state. A change in any of these rates will change the relative amount of either species. By altering the experimental conditions under which the time-resolved emission spectra are obtained, evidence may be provided for other excited-state reactions such as excimer formation, exciplex formation, or solvent relaxation occurring on the same time scale.

Quantitation of the rate of interconversion of the excited-state species results from analysis of decay curves at wavelengths where emission is due to only one species. Several conceptually different methods can be used to calculate the rate of proton transfer. Analysis of the lifetimes of the species in specific pH regions, analysis of the change in relative inten-

sities of the species at various times during the fluorescence decay, or analysis of the specific exponential character of the decay curves can all yield the rates of transformation. In carrying out the calculations by a number of different methods, the values obtained may be used as a check on the consistency of the proposed kinetic scheme. In this way the model for the reaction is either further substantiated or shown to be incorrect. The manner in which the various answers deviate from each other may suggest new models which can be further tested.

A. Difference of Lifetimes of Single Exponentials. The rate equations that describe the kinetic scheme in Figure 1 can be written as

$$-\mathrm{d}[A^*]/\mathrm{d}t = (k_{F1A} + k_{QA} + k_F)[A^*] - k_R[H^+][B^*] \quad (1)$$

$$-\mathrm{d}[B^*]/\mathrm{d}t = (k_{F1B} + k_{QB} + k_R[H^+])[B^*] - k_F[A^*] \quad (2)$$

At pH values much less than the excited-state pK, no ionization occurs and eq 1 reduces to eq 3. The integrated form of

$$-\mathrm{d}[A^*]/\mathrm{d}t = (k_{F1A} + k_{QA})[A^*] \quad (3)$$

this equation describing the fluorescence decay is a single exponential with a lifetime of $1/(k_{F1A} + k_{QA})$. This situation is obtained in the 2-naphthol system at pH values of zero or less.

Near the excited-state pK (for 2-naphthol, pH values of 2–4) eq 1 describes the fluorescence decay of the protonated form which can be described by a sum of two exponentials. As the hydrogen ion concentration is decreased, the second term on the right side of eq 1 becomes negligible (for 2-naphthol, pH values of 4–7), and the equation becomes

$$-\mathrm{d}[A^*]/\mathrm{d}t = (k_{F1A} + k_{QA} + k_F)[A^*] \quad (4)$$

The decay is again described by a single exponential now with a lifetime of $1/(k_{F1A} + k_{QA} + k_F)$.

Assuming k_{QA} is independent of the hydrogen ion concentration, k_F can be obtained from the difference between the reciprocals of the lifetimes of the protonated species under the conditions specified by eq 3 and 4. The lifetimes of fluorescence decay curves of 2-naphthol collected at pH 5.5 and 0.3 were 5.26 and 6.76 nsec, respectively, yielding a value of 4.2×10^7 sec^{-1} for k_F. An estimation of k_R can be made from a calculation of the excited state pK (Förster, 1950a,b) and the k_F value obtained by these lifetime measurements.

B. Instantaneous Derivative-Intensity Graphs. A second method of calculating rate constants is based on a rearrangement of the original rate equations. Dividing eq 1 by [A*] and eq 2 by [B*] yields

$$-\mathrm{d}[A^*]/\mathrm{d}t/[A^*] = (k_{F1A} + k_{QA} + k_F) - k_R[H^+][B^*]/[A^*] \quad (5)$$

$$-\mathrm{d}[B^*]/\mathrm{d}t/[B^*] = (k_{F1B} + k_{QB} + k_R[H^+]) - k_F[A^*]/[B^*] \quad (6)$$

Since fluorescence lifetime techniques measure the time-dependent changes in intensity rather than concentration, it is necessary to introduce the proper proportionality factors relating intensity to concentration and, therefore, to the rates (eq 7 and 8).

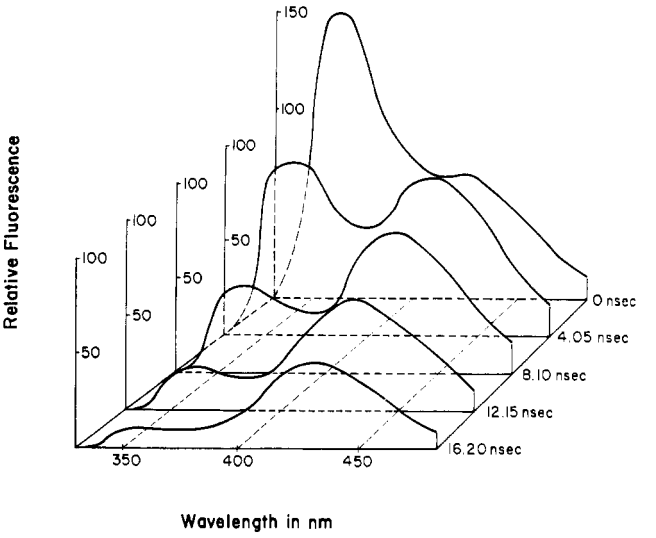

FIGURE 3: Nanosecond time-resolved emission spectra of 10^{-4} M 2,6-naphtholsulfonate with the rate of excited-state ionization slowed by the addition of 40% ethanol. Fluorescence decay curves at any particular wavelength can be regenerated by connecting the spectra at that wavelength.

$$-\mathrm{d}I_A/\mathrm{d}t/I_A = (k_{F1A} + k_{QA} + k_F) - k_R[H^+]I_BC_B/I_AC_A \quad (7)$$

$$-\mathrm{d}I_B/\mathrm{d}t/I_B = (k_{F1B} + k_{QB} + k_R[H^+]) - k_FI_AC_A/I_BC_B \quad (8)$$

The proportionality constants, C_A and C_B, are dependent on instrumental sensitivity factors, on emission probabilities at specific wavelengths, and on the natural lifetimes of the excited states. The ratio of C_A to C_B can be experimentally obtained as outlined in Appendix A.

Experimental values of the intensities from fluorescence decay curves and the instantaneous derivative of these intensities can be substituted into eq 7 and 8. The rate constants for proton transfer can then be calculated by solving these equations using the appropriate proportionality factors.

Fluorescence decay curves for the naphthol system were obtained at 360 nm for the protonated form and 450 nm for the ionized form (Figure 4A). These curves were normalized to a constant lamp intensity and a blank was substracted from the curves collected at 360 nm. The instantaneous derivative at each time on these curves was calculated by fitting nine consecutive points to a second-order polynomial and by calculating the derivative for the central point. The interval of calculation was then successively shifted along the decay curve one point at a time and the derivative was evaluated (Figure 4B).

These experimental derivative values along with the fluorescence intensities at each time were substituted into eq 7 and 8, and the data were plotted as shown in Figures 5 and 6. The first few data points of the derivative-intensity plot for the $\mathrm{d}I_A/\mathrm{d}t$ curve (Figure 5) do not lie on a straight line because the fluorescence decay function is convolved with a lamp flash of finite width. It can be shown by computer simulation that the slope and intercept of the straight-line segment through the data taken *after* the lamp flash do not differ significantly from those expected had the lamp flash approximated a Δ function. The derivative-intensity graph for the $\mathrm{d}I_B/\mathrm{d}t$

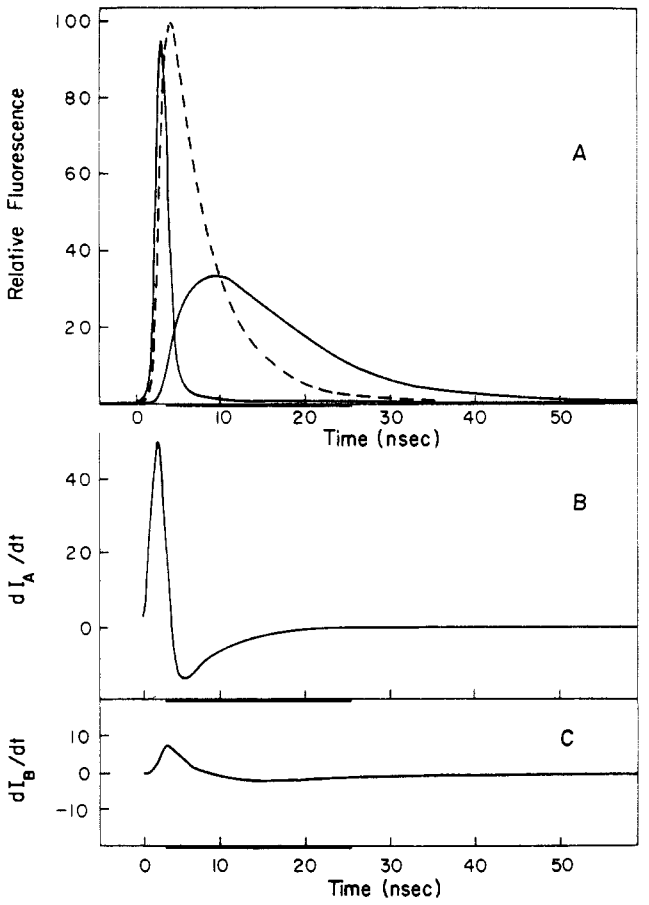

FIGURE 4: (A) Fluorescence decay curves of 2-naphthol at pH 3.43. The sharp peak represents the decay profile of the lamp flash intensity. The dashed line is the decay profile of naphthol collected at 360 nm. The curve shifted furthest right is the decay profile of naphtholate collected at 450 nm and magnified 2.5 times relative to the 360 nm curve. (B) Instantaneous derivative curves of the intensities of napthol and (C) naphtholate. The heavy line on the time axis indicates the portion of the curves used in the derivative-intensity graphs (Figures 5 and 6).

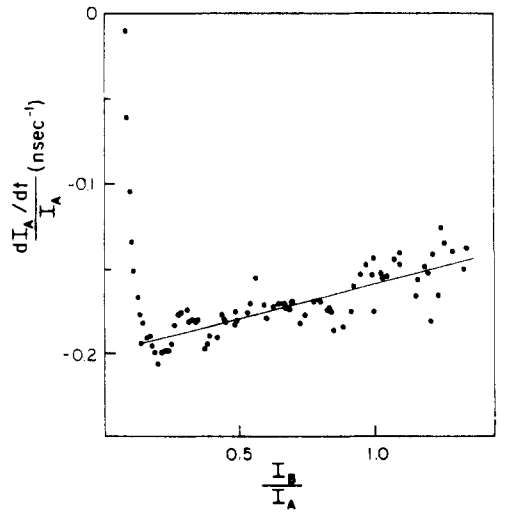

FIGURE 5: Derivative-intensity plot of 2-naphthol at pH 3.43 using the derivative of the protonated naphthol. Data at low values of I_B/I_A did not fall on a straight line because of convolution and were not used in the calculations. The slope of the least-squares fit of the selected data yielded $k_R = 7.9 \pm 0.6 \times 10^{10}$ M^{-1} sec^{-1} and an intercept $(k_{F1A} + k_{QA} + k_F) = 0.20 \pm 0.01$ nsec^{-1}.

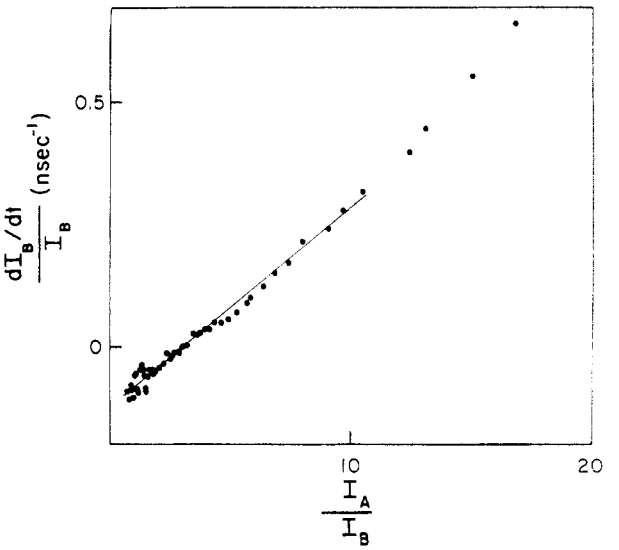

FIGURE 6: Derivative-intensity plot of 2-naphthol at pH 3.43 using the derivative of the naphtholate. Data at high values of I_A/I_B did not fall on a straight line because of convolution and were not used in the calculations. The slope of the least-squares fit of the selected data yielded $k_F = 5.1 \pm 0.1 \times 10^7$ sec^{-1} and an intercept $(k_{F1B} + k_{QB} + k_R[H^+]) = 0.13 \pm 0.02$ nsec^{-1}.

curve (Figure 6) is not greatly affected by convolution. The data points at high A/B values, however, do deviate slightly from a straight line and have not been used in the computations.

The slope of the line in Figure 5 is equal to $k_R[H^+](C_B/C_A)$, while the intercept is the sum of the rate constants $k_{F1A} + k_{QA} + k_F$. The slope of the line in Figure 6 is equal to $k_F \cdot (C_A/C_B)$, while the intercept is the sum of the rate constants $k_{F1B} + k_{QB} + k_R[H^+]$. Values of k_F and k_R obtained from the slopes of the least-squares fits of these data were 5.1×10^7 sec^{-1} and 7.9×10^{10} M^{-1} sec^{-1}. Data collected before the lamp intensity decreased to 10% of its maximum value were not used in the calculations.

The intercept of the derivative-intensity plot using eq 8 is equal to $k_{F1B} + k_{QB} + k_R[H^+]$. A replot of these intercepts as a function of hydrogen ion concentration produces a straight line with an intercept of $k_{F1B} + k_{QB}$ (Figure 7). The value of k_R obtained from the slope of a least-squares fit of this plot was found to be 5.0×10^{10} M^{-1} sec^{-1}.

As a result of the effect of convolution and the manner in which greater weight is placed on those points with the great-

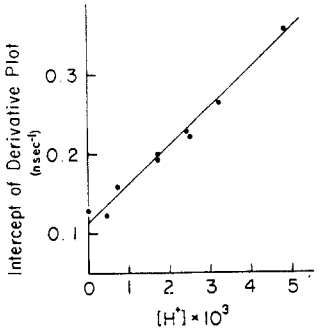

FIGURE 7: Intercepts of derivative-intensity graphs (dI_B/dt) plotted as a function of $[H^+]$. The least squares fit yielded a slope $k_R = 5.0 \pm 0.2 \times 10^{10}$ M^{-1} sec^{-1} and an intercept $(k_{F1B} + k_{QB}) = 0.11 \pm 0.01$ nsec^{-1}.

TABLE I: Analysis of Decay Curves by the Method of Moments.

		450 nm				360 nm			
pH	$[H^+] \times 10^8$	γ_1 ($nsec^{-1}$)	γ_2 ($nsec^{-1}$)	A_1	A_2	γ_1 ($nsec^{-1}$)	γ_2 ($nsec^{-1}$)	A_1	A_2
2.32	4.8	0.431	0.143	−0.371	0.372	0.467	0.145	0.303	0.754
2.62	2.4	0.282	0.145	−0.712	0.744	0.242	0.137	0.813	0.484
2.76	1.7	0.287	0.124	−1.07	1.09	0.314	0.124	1.26	0.687
3.15	0.71	0.281	0.107	−1.20	1.16	0.296	0.116	0.540	0.191
3.43	0.37	0.225	0.122	−1.43	1.46	0.224	0.079	1.98	0.011

est amount of noise, calculations using $(dI_A/dt)/I_A$ have concomitantly greater uncertainty than those obtained from the $(dI_B/dt)/I_B$ graph. Since it is possible to calculate all of the rate constants from the dI_B/dt plot, the calculation from dI_A/dt curves is used as an internal control to check consistency.

The linearity of the data presented in Figure 7 verifies the earlier assertion that k_{QB} does not change over a wide pH range. This observation was further substantiated in a separate experiment in which the lifetime of the naphtholate emission was determined at pH 11.4. At this pH the fluoresecnce decay is characterized by a single exponential with a lifetime of $1/(k_{F1B} + k_{QB})$. The measured lifetime of 9.7 nsec is in good agreement with the value of 9.1 nsec calculated from the reciprocal of the least-squares intercept of Figure 7.

Under conditions where the hydrogen ion concentration cannot be changed, *i.e.*, when the chromophore is bound to a protein, both the dI_A/dt and the dI_B/dt curves must be used. Besides being able to calculate k_F and k_R using both derivative-intensity graphs, a determination of a change in k_Q can be made subject to the constraint that k_{F1A} and k_{F1B} do not change upon binding. The intercepts of these derivative-intensity graphs contain the quantities $k_{F1A} + k_{QA}$ and $k_{F1B} + k_{QB}$. A comparison of the calculated value for the intercept to that obtained experimentally gives a quantitative measure of the change in k_Q under a particular set of experimental conditions.

C. Exponential Analysis of Decay Curves. A third method of calculation involving the analysis of the exponential character of the individual fluorescence decay curves can also yield these same rate constants. Integration of eq 1 and 2 subject to the initial boundary conditions $[A^*] = [A_0^*]$, $[B^*] = 0$, at $t = 0$, yields

$$[A^*] = \frac{[A_0^*]}{(\gamma_2 - \gamma_1)}[(\gamma_2 - X)e^{-\gamma_1 t} + (X - \gamma_1)e^{-\gamma_2 t}] \quad (9)$$

$$[B^*] = \frac{k_F[A_0^*]}{(\gamma_2 - \gamma_1)}[e^{-\gamma_1 t} - e^{-\gamma_2 t}] \quad (10)$$

where $\gamma_{1,2} = 1/2[(X + Y) \pm \{(Y - X)^2 + 4k_F k_R[H^+]\}^{1/2}]$ and $X = (k_{F1A} + k_{QA} + k_F)$ and $Y = (k_{F1B} + k_{QB} + k_R \cdot [H^+])$.

Equations 9 and 10 are of the same form as the equations given by Birks (1970) for excimer formation. The decay of the protonated species is the sum of two exponentials each with different amplitude factors. The decay of the ionized species is the difference of two exponentials, the amplitudes of which are equal in magnitude but opposite in sign. The exponents for the two curves should be identical.

The experimentally obtained decay curves were analyzed for two exponential components using the method of moments as adapted by Isenberg and Dyson (1969). This method of analysis yields both amplitude and exponential factors for the experimental curves. Analysis of exponential decay curves appears to be extremely sensitive to nonrandom noise. Data which did not meet specific criteria after this analysis were rejected. These criteria were that the decay curves of the ionized species must have amplitude factors which are equal in magnitude and opposite in sign, while both protonated and ionized decay curves for a single experiment must yield comparable exponential terms (eq 9 and 10).

The results obtained from analyses of decay curves at different pH are given in Table I. The amplitude factors, A_1 and A_2, obtained for the decay curves at 450 nm (ionized species) are equal in magnitude yet opposite in sign. The exponential terms, γ_1 and γ_2, are the same for the two wavelengths at a given pH. The largest deviation is 15% with the exception of γ_2 at pH 3.43. It should be noted that the amplitude factor at this pH for the second component is only 7% of the total emission, so that a degree of uncertainty is expected.

The sum of the exponents from the method of moments calculation, $\gamma_1 + \gamma_2$, is equal to the sum $k_{F1A} + k_{QA} + k_F + k_{F1B} + k_{QB} + k_R[H^+]$. The reverse rate constant can be calculated by plotting $\gamma_1 + \gamma_2$, obtained from either the ionized or protonated decay curves, as a function of hydrogen ion concentration. The most reproducible and consistent data for $\gamma_{1,2}$ came from analysis of the fluorescence decay curves of the ionized species. Data obtained for 2-naphthol yielded a straight line with a slope of k_R equal to $4.5 \times 10^{10}\ M^{-1}\ sec^{-1}$ (Figure 8). This graph is almost identical with the graph of intercepts of the derivative-intensity curves plotted *vs.* hy-

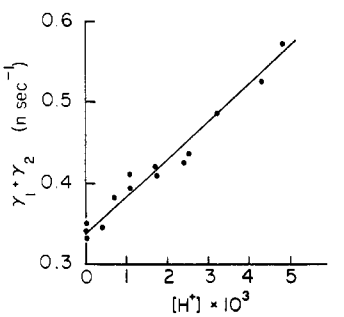

FIGURE 8: Sum of the exponents of the method of moments analysis of the decay curves as a function of $[H^+]$. The least-squares fit of the data yielded a slope $k_R = 4.5 \pm 0.3 \times 10^{10}\ M^{-1}\ sec^{-1}$ and an intercept $(k_F + k_{F1A} + k_{QA} + k_{F1B} + k_{QB}) = 0.31 \pm 0.06\ nsec^{-1}$.

drogen ion concentration (Figure 7), thereby showing the consistency between the two conceptually different methods.

The forward rate constant can be calculated from a combination of the amplitude and exponential factors of the integrated rate equations (eq 9 and 10). The sum of the amplitude factors obtained from the decay curve of the protonated species described by eq 9 is equal to

$$\text{amplitude } A_1 + \text{amplitude } A_2 = \frac{[A_0^*](\gamma_2 - X)}{(\gamma_2 - \gamma_1)} + \frac{[A_0^*](X - \gamma_1)}{(\gamma_2 - \gamma_1)} = [A_0^*] \qquad (11)$$

This relative $[A_0^*]$ can be substituted into the amplitude factor of eq 10.

$$\text{amplitude } |B| = \frac{k_F[A_0^*]}{(\gamma_2 - \gamma_1)} = \frac{k_F}{(\gamma_2 - \gamma_1)} [\text{amplitude } A_1 + \text{amplitude } A_2] \qquad (12)$$

The amplitudes, A_1, A_2, and $|B|$, of the actual fluorescence intensity decay curves can be substituted into eq 12 using the appropriate proportionality factors, C_A and C_B. Experimentally these amplitudes and the exponential terms γ_1 and γ_2 are obtained by the method of moments analysis of decay curves corrected to the same exciting light flux. The value of k_F is then obtained from eq 13. The average value of k_F for 2-

$$k_F = \frac{C_B}{(C_A)} \frac{(\text{amplitude } |B|)(\gamma_2 - \gamma_1)}{\text{amplitude } A_1 - \text{amplitude } A_2} \qquad (13)$$

naphthol obtained by this method of analysis was 4.8×10^7 sec^{-1}.

Conclusion

Calculations of rates of excited-state proton transfer have previously been made using steady-state techniques (Weller, 1952, 1961; Trieff and Sundheim, 1965). In this method the relative quantum yields of the protonated and ionized species are determined as a function of pH. In addition to the steady-state measurements, fluorescence lifetimes must also be known or assumed in order to complete the calculations. The accuracy of the steady-state method is dependent on the accuracy of the quantum yield measurements and the accuracy of the determination of the overlap of the two emission spectra. One requirement of this method is that there must be no pH-dependent rate of quenching. The sum of the two relative quantum yields must equal a constant value. It is also necessary to assume that proton transfer follows the prescribed kinetic scheme. Time-dependent changes in the rates of quenching, excimer formation, solvent relaxation, or time-dependent changes in the rates of transfer themselves cannot be detected by this method.

The calculation of rates from kinetic data has many advantages over the steady-state methods. The situation is analogous to the relation between steady-state kinetic studies of enzymes and the more detailed information often available from flow or relaxation investigations. The methods described in this paper are more direct than the steady-state methods since they utilize the information present in the fluorescence decay curves themselves. These lifetime measurements can generally be made with more accuracy than is possible with quantum-yield measurements (Ware, 1971). The requirement that rates of quenching do not change with changes in experimental parameters does not have to be met. In fact, if there is a change in a quenching rate, its magnitude can be determined.

One significant advantage of nanosecond fluorometry is the potential of identifying a system which is not consistent with a proposed mechanism. Time-resolved emission spectra are useful for detecting processes such as solvent relaxation, exciplex formation, or excimer formation. If such reactions take place on the same time scale as the fluorescence decay, they will show up as time-dependent shifts in emission maxima. In addition such processes will lead to deviations from linearity in the derivative intensity plots. There will also be inconsistencies in the relations between the amplitudes and exponential terms of the decay curves as determined by the method of moments. The nature of the deviations may suggest other mechanisms which can be tested.

Three methods of analysis are described here. Method A (differences of lifetimes of single exponentials) is conceptually similar to the steady-state approach. It has the same inherent requirement that k_Q is constant, and it compares a value obtained at an intermediate pH to that obtained at an extreme pH. It does have the advantage that systems which have time-dependent changes in rate constants will not give single exponential decay curves, suggesting that other mechanisms must be invoked. This method, like the steady-state method, cannot be used to calculate k_R directly. It cannot be used for calculations with probes on proteins unless the rate is such that a single exponential curve is obtained. The assumption of a constant k_Q would still have to be made. This method does provide a rapid way to determine the forward, and indirectly, the reverse rate constants in an aqueous solution.

Method B (instantaneous derivative-intensity graph) uses information from decay curves of *both* the ionized and protonated species. It is not dependent on fitting exponential curves to experimental data; rather it depends on the relative intensities and changes in intensities at specific times during the fluorescence decay. It is necessary to determine C_A and C_B, the proportionality constants for converting relative intensities to relative concentrations of excited species. The calculation of rate constants using the derivative method seems to be the least susceptible to errors due to noise. It not only allows for the calculation of k_F and $k_R[H^+]$, as well as k_{QA} and k_{QB}, but these calculations can be made without varying the pH. This is a requirement for the calculation of rates of proton transfer on proteins. An important aspect of this type of analysis is that a check can be made to determine whether the experimental data are consistent with the kinetic scheme.

Method C (exponential analysis of decay curves) analyzes the data in terms of a sum or difference of two exponentials which are then related, by presupposing a kinetic scheme, to specific rate constants. Inability to fit the data to a scheme may be construed to be due to a deviation from that scheme or it may be a result of the inherent difficulty in evaluating two amplitudes and two exponential terms from a noisy decay curve convolved with a noisy lamp flash. In fact it is not always possible to ascertain whether the decay is described by two exponential terms or whether more exponential terms are required. The calculation of k_R using this method is dependent upon changing the hydrogen ion concentration; however, k_F can be determined from the amplitudes of one set of decay curves. The value of k_R could be calculated indirectly from the excited state pK. It should be noted that the equations have been solved with the boundary conditions of $[B^*] = 0$ at

time = 0, a situation which may not be attained under certain experimental conditions.

The forward and reverse rate constants for excited-state proton transfer obtained from several experiments for 2-naphthol in water by the three lifetime techniques and by the steady-state approach are summarized in Table II. There is

TABLE II

	k_F (sec^{-1})	k_R (M^{-1} sec^{-1})
Determinations by Weller	4.1×10^7	5.1×10^{10}
Difference of lifetimes	4.2×10^7	5.1×10^{10}
Method of moments	4.8×10^7	5.0×10^{10}
Derivative	5.1×10^7	5.0×10^{10}

good agreement between the values obtained by the various methods outlined in this paper and the steady-state data of Weller (1952). Calculations of rates of proton transfer of 2,6-naphtholsulfonate adsorbed to bovine serum albumin could not be made. The changes in the rates of ionization of the bound chromophore as compared to the dye in aqueous solution are so great that no excited-state proton transfer is observed. In order for this type of probe to be used quantitatively some excited-state ionization must be detectable. The 2,6-naphtholsulfonate–bovine serum albumin complex does demonstrate the dramatic change which can be observed when the environment of such a dye is changed.

Since rates of excited-state proton transfer depend on the character of the solvent as well as on the nature of the proton acceptor (Stryer, 1966; Trieff and Sundheim, 1965; Deluca *et al.*, 1971), localized changes in these parameters which occur when a macromolecule undergoes conformational change may be reflected by changes in these rates. Fluorescent probes which undergo excited-state ionization can thus be used both for the characterization of their microenvironments and as sensitive detectors of conformational changes. Extrinsic probes similar to 2-naphthol or its derivatives can be designed which will bind covalently or be adsorbed to selected sites of interest on biological macromolecules. Tyrosine, an intrinsic probe, might also be valuable since it is known to undergo excited-state proton transfer (Feitelson, 1964; Weber and Rosenheck, 1964). This method then provides a new, quantitative application of fluorescence in the study of biological systems.

Acknowledgments

We thank Dr. Robert Schuyler for help with instrumentation and modification of the method of moments program for the H.P. 2100 computer. We thank Drs. R. D. Dyson and I. Isenberg for making their program on the method of moments available to us. Rex Hjelm kindly assisted us in writing the program to perform the numerical differentiation.

Appendix A

The ratio of C_A to C_B can be experimentally obtained from decay curves under conditions where only one excited-state species exists. For the naphthols one set of data is collected at pH 0 where only the protonated species is present, while another set of data is collected at pH 11.4 where only the naphtholate is present. The integrated rate equations for these two solutions can be written as

$$[A^*] = [A_0^*]e^{-t/\tau_A} = (I_{A0})C_A e^{-t/\tau_A} \quad (14)$$

$$[B^*] = [B_0^*]e^{-t/\tau_B} = (I_{B0})C_B e^{-t/\tau_B} \quad (15)$$

The ratio of C_A to C_B is determined from the amplitude factors of these equations. The ratio of the number of molecules initially placed in the excited state is equal to the ratio of the light absorbed by these two solutions. The relative light

$$[A_0^*]/[B_0^*] = \text{relative light absorbed by A}/\text{relative light absorbed by B} \quad (16)$$

absorbed by the two solutions can be calculated from the spectral output of the exciting lamp after passage through an interference filter and from the absorption spectra of the solutions over the range of transmission of the filter. This can be expressed as

$$\text{relative light absorbed} = \int_{\lambda_1}^{\lambda_2} I(\lambda)OD(\lambda)d\lambda \quad (17)$$

where $OD(\lambda)$ is the sample absorbance and $I(\lambda)$ is the relative photon flux incident on the cuvet after passage through the interference filter with significant transmission only in the spectral region λ_1 to λ_2.

Relative values for I_{A_0} and I_{B_0} can be obtained for these same solutions normalized to the same light intensity from an analysis using the method of moments. A calculation of the ratio C_A/C_B can then be made from eq 18.

$$\frac{\text{relative light absorbed by A}}{\text{relative light absorbed by B}} = (I_{A_0})C_A/(I_{B_0})C_B \quad (18)$$

The ratio of the proportionality factors C_A/C_B for 2-naphthol was found to be 1.26. The decay curve for the protonated form was collected at 360 nm while that of the ionized form was collected at 450 nm.

References

Birks, J. B. (1970), Photophysics of Aromatic Molecules, New York, N. Y., John Wiley, p 304.

Bowie, L., Irvin, R., and DeLuca, M. (1972), *Fed. Proc., Fed. Amer. Soc. Exp. Biol. 31*, 420 Abstr.

Brand, L., and Gohlke, J. R. (1971), *J. Biol. Chem. 246*, 2317.

Brand, L., Gohlke, J. R., and Rao, D. S. (1967), *Biochemistry 6*, 3510.

Coates, P. B. (1968), *J. Sci. Instrum. 1*, 878.

DeLuca, M., Brand, L., Cebula, T. A., Seliger, H. H., and Makula, A. F. (1971), *J. Biol. Chem. 246*, 6702.

Feitelson, J. (1964), *J. Phys. Chem. 68*, 391.

Förster, Th. (1950a), *Z. Elektrochem. 54*, 42.

Förster, Th. (1950b), *Z. Elektrochem. 54*, 531.

Gohlke, J. R. (1971), Ph.D. Dissertation, The Johns Hopkins University.

Isenberg, I., and Dyson, R. D. (1969), *Biophys. J. 9*, 1337.

Loken, M. R., Hayes, J. W., Gohlke, J. R., and Brand, L. (1972), *Fed. Proc., Fed. Amer. Soc. Exp. Biol. 31*, 470 Abstr.

Schuyler, R., and Isenberg, I. (1971), *Rev. Sci. Instrum. 42*, 813.

Stryer, L. (1966), *J. Amer. Chem. Soc. 88*, 5708.
Trieff, N. M., and Sundheim, B. R. (1965), *J. Phys. Chem. 69*, 2044.
Vander Donckt, E. (1970), *Progr. React. Kinet. 5*, 273.
Ware, W. (1971), *in* Creation and Detection of the Excited State, Lamola, A. A., Ed., New York, N. Y., Marcel Dekker, p 213.
Weber, G., and Rosenheck, K. (1964), *Biopolym. Symp. 1*, 333.
Wehry, E. L., and Rogers, L. B. (1966), *in* Fluorescence and Phosphorescence Analysis, Hercules, D. M., Ed., New York, N. Y., Interscience, p 81.
Weller, A. (1952), *Z. Elektrochem. 56*, 662.
Weller, A. (1961), *Progr. React. Kinet. 1*, 187.

Structure of the Carbon Monoxide Binding Site of Hemocyanins Studied by Fourier Transform Infrared Spectroscopy†

Lei Yen Fager and James O. Alben*

ABSTRACT: Carbon monoxide complexes of hemocyanin from several sources have been studied by infrared spectroscopy. The CO stretching vibrations (νCO) for two molluscs (squid and limpet) occur near 2063 cm^{-1}, at 2054 cm^{-1} for the horseshore crab (*Limulus*) and near 2043 cm^{-1} for two crustaceans (Atlantic rock crab and Ohio crayfish). These frequencies are clear evidence of different local molecular environments for bound CO in hemocyanins from these three groups, and support our proposal that the proteins provide different ligands to coordinate to copper at the active site. The isotopic shift (ν^*/ν) for [^{18}C]carbon monoxide bound to hemocyanin is nearly identical with that for the free gas, while ν^*/ν for [^{18}O]-carbon monoxide bound to hemocyanin is less than that for the free gas for all animal sources except crayfish, which was not tested. These data rule out all model structures in which CO is bridged between two copper atoms or in which the CO is bound perpendicular to a line through the copper nucleus. They are consistent with a structure in which the oxygen atom of CO is coordinated to one atom of copper. A model for the hemocyanin carbonyl complex is proposed which includes a trigonal oxygen of CO coordinated to one copper atom (C–O–Cu angle near 120°), with the second copper atom of the binding site coordinated only to protein.

Complexes of small molecules with heme proteins have been studied in great detail, but relatively little is known about ligand binding to copper proteins. We have therefore undertaken a study of carbon monoxide complexes of hemocyanins from several species. Hemocyanins are the oxygen transport proteins in the hemolymph of many molluscs and decapod crustaceans, and reversibly bind oxygen or carbon monoxide with a stoichiometry of one ligand per two copper atoms (Redfield *et al.*, 1928a; Root, 1934; Kubowitz, 1938; Vanneste and Mason, 1966; Rocca and Ghiretti, 1963). This stoichiometry led to speculation that the ligand might form a bridging structure between two atoms of copper, and Williams (1966) listed possible bridging structures for carbon monoxide bound

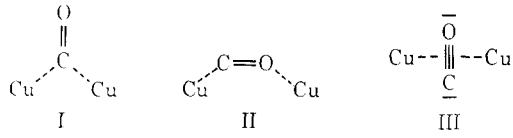

I II III

to copper. In a preliminary study, Alben *et al.* (1970) found only a single narrow absorption band due to carbon monoxide bound to hemocyanin from the giant keyhole limpet (*Megathura crenulata*) at a frequency (2063 cm^{-1}) which is consistent with a nonbridging copper carbonyl structure, but which is too high for structures I or II. The frequency of this absorption band was similar to that observed (2069 cm^{-1}, Alben *et al.*, 1970) for copper carbonyl in pyridine solution which is known to be a nonbridging carbonyl coordinated to a single copper (Manchot and Friend, 1908; Wagner, 1931). No bridging carbonyl complexes of copper are known, but they are common for binuclear complexes of iron or cobalt. Absorptions of bridging carbonyls in these complexes are observed in the range of 1800–1900 cm^{-1}, whereas mononuclear complexes are generally observed from about 1950 to 2150 cm^{-1} (Nakamoto, 1963). The range of frequencies is caused by the variety of ligands coordinated to the metal, and to the net charge on the complex. It has been amply demonstrated (Bigorgne, 1961; Bouquet *et al.*, 1968; Alben and Caughey, 1968) that electron-withdrawing effects of ligands are transmitted through a coordinated metal to ligands such as CO, which are coordinated to the same metal. Structure III was not tested by these data, but is ruled out by data presented in this paper.

The nature of ligands coordinated to the metal in copper proteins has been of interest for many years, but has been difficult to determine since any chemical or conformational change in the protein may lead to ligand exchange by the copper, and copper(I) is diamagnetic and not observed by electron spin resonance. Others have speculated that sulfhydryl (Klotz and Klotz, 1955) or histidyl (Lontie, 1958) residues may be coordinated in hemocyanins. We present evidence from the

† From the Department of Physiological Chemistry, Ohio State University, College of Medicine, Columbus, Ohio 43210. *Received May 15, 1972.* Supported by Research Grant GM 11067 from the U. S. Public Health Service, and by a contract from the Department of the Air Force.